Z. Angew. Math. Phys. (2017) 68:75

0044-2275/17/030001-16
published online May 30, 2017
DOI 10.1007/s00033-017-0819-3

Zeitschrift für angewandte Mathematik und Physik ZAMP

Axisymmetric planar cracks in finite hollow cylinders of transversely isotropic material: Part II—cutting method for finite cylinders

M. Pourseifi, R. T. Faal and E. Asadi

Abstract. This paper is the outcome of a companion part I paper allocated to finite hollow cylinders of transversely isotropic material. The paper provides the solution for the crack tip stress intensity factors of a system of coaxial axisymmetric planar cracks in a transversely isotropic finite hollow cylinder. The lateral surfaces of the hollow cylinder are under two inner and outer self-equilibrating distributed shear loadings. First, the stress fields due to these loadings are given for both infinite and finite cylinders. In the next step, the state of stress in an infinite hollow cylinder with transversely isotropic material containing axisymmetric prismatic and radial dislocations is extracted from part I paper. Next, using the distributed dislocation technique, the mixed mode crack problem in finite cylinder is reduced to Cauchy-type singular integral equations for dislocation densities on the surfaces of the cracks. The problem of a cracked finite hollow cylinder is treated by *cutting method*; i.e., the infinite cylinder is cut to a finite one by slicing it using two annular axisymmetric cracks at its ends. The cutting method is validated by comparing the state of stress of a sliced intact infinite cylinder with that of an intact finite cylinder. The paper is furnished to several examples to study the effect of crack type and location in finite cylinders on the ensuing stress intensity factors of the cracks and the interaction between the cracks.

Mathematics Subject Classification. 74A45.

Keywords. Axisymmetric cracks, Mixed mode fracture, Dislocation, Finite hollow cylinder, Transversely isotropic material.

1. Introduction

The introduction of the present study (including two companion part I and part II papers) is provided in the part I paper. This paper deals with the in-plane analysis of cracks and is organized as follows. The purpose of this paper is to formulate a mixed mode fracture analysis for a finite cylinder with multiple cracks. The finite cylinder is weakened by axisymmetric penny-shaped, annular, and circumferential edge cracks. To the best of the authors' knowledge, the mixed mode problem of finite cylinder with multiple axisymmetric interacting cracks was not investigated before. This problem is solved by introducing a novel method namely "cutting method." First, we use the fundamental prismatic and radial dislocation solution for an infinite hollow cylinder with transversely isotropic material which is given in part I of the paper. Next, we employ the dislocation solution to analyze related crack problems in a finite hollow cylinder using cutting method. That is, a similar cracked infinite hollow cylinder is sliced by extending two additional annular axisymmetric cracks. The related problem is solved by distributing edge dislocation obtained for an infinite hollow cylinder. In fact, the number of the defects in a cracked infinite cylinder is only two more than those in a cracked finite cylinder and the additional defects are two extended ring crack to cut the infinite cylinder.

Analytical solutions of the intact infinite/finite cylinders under shear stresses on their inner and outer surfaces are presented in Sect. 2. The cutting method was introduced in Sect. 3 and is used to analyze a finite hollow cylinder with multiple axisymmetric planar cracks. By employing the dislocation solution of the part I of the paper, the ensuing Cauchy-type singular integral equations for the hollow finite cylinder weakened by several axisymmetric planar cracks are formulated and solved. Section 4 presents numerical

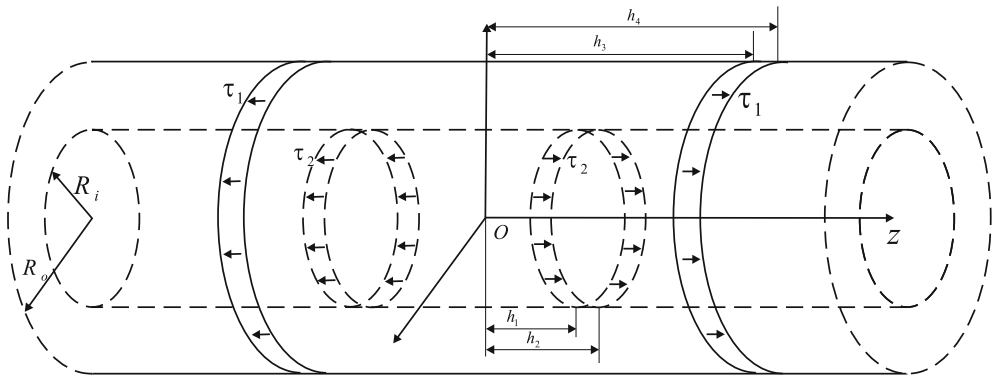

FIG. 1. An infinite hollow cylinder under two pair of self-equilibrating shear stresses

examples to study the effect of loading, material anisotropy, and interaction of cracks on the resulting stress intensity factors at the crack tips. Section 5 offers concluding remarks.

2. Solution of an intact cylinder under shear stresses on its inner and outer surfaces

2.1. An infinite cylinder under two self-equilibrating shear stresses on inner and outer surfaces

First, we consider an intact infinite hollow cylinder in which its outer surface subjected to a pair of self-equilibrating shear stresses as $\sigma_{rz}(R_o,z)=\tau_1\left[H(z-h_3)-H(z-h_4)\right], h_3<h_4$ and $\sigma_{rz}(R_o,z)=\tau_1\left[H(z+h_3)-H(z+h_4)\right]$ as shown in Fig. 1.

Also we consider another pair of self-equilibrating shear stresses applying to the outer surface of the cylinder as $\sigma_{rz}(R_i,z)=\tau_2\left[H(z-h_1)-H(z-h_2)\right], h_1<h_2$ and $\sigma_{rz}(R_i,z)=\tau_2\left[H(z+h_1)-H(z+h_2)\right]$.

This problem is also symmetric with respect to the plane $z=0$. Satisfying the boundary conditions along the inner and outer surfaces of the cylinder for $z>0$ implies that

$$\begin{aligned}&\sigma_{rr}(R_o,z)=0,\quad \sigma_{rr}(R_i,z)=0\\&\sigma_{rz}(R_o,z)=\tau_1\left[H(z-h_3)-H(z-h_4)\right]\\&\sigma_{rz}(R_i,z)=\tau_2\left[H(z-h_1)-H(z-h_2)\right]\end{aligned}\tag{1}$$

To solve the problem we employ the solution form (6) and also the resultant displacement and stress field (8) of part I of the paper. Since the number of boundary conditions is four, we eliminate the coefficients $E(\eta)$ and $F(\eta)$. The boundary conditions (1) are applied to Eq. (8) of part I of the paper by means of the Fourier sine transform of the Heaviside step function, i.e., $H(z-h_k)=\frac{2}{\pi}\int_0^\infty\frac{1}{\xi}\cos(h_k\xi)\sin(z\xi)\,\mathrm{d}\xi, k=1,2$, gives

$$\begin{aligned}&A(\xi)\left[\varrho_5 I_0(R_i\xi\varrho_1)-(b-1)\frac{\varrho_1}{R_i\xi}I_1(R_i\xi\varrho_1)\right]\\&+B(\xi)\left[\varrho_5 K_0(R_i\xi\varrho_1)+(b-1)\frac{\varrho_1}{R_i\xi}K_1(R_i\xi\varrho_1)\right]\\&+C(\xi)\left[\varrho_6 I_0(R_i\xi\varrho_2)-(b-1)\frac{\varrho_2}{R_i\xi}I_1(R_i\xi\varrho_2)\right]\\&+D(\xi)\left[\varrho_6 K_0(R_i\xi\varrho_2)+(b-1)\frac{\varrho_2}{R_i\xi}K_1(R_i\xi\varrho_2)\right]=0\end{aligned}$$

$$
\begin{aligned}
&-\frac{2}{\pi}\int_0^\infty \xi[A(\xi)\varrho_1\varrho_5 I_1(R_i\xi\varrho_1) - B(\xi)\varrho_1\varrho_5 K_1(R_i\xi\varrho_1)\\
&+C(\xi)\varrho_2\varrho_6 I_1(R_i\xi\varrho_2) - D(\xi)\varrho_2\varrho_6 K_1(R_i\xi\varrho_2)]\sin(z\xi)\,\mathrm{d}\xi\\
&=\frac{2\tau_2}{\pi}\int_0^\infty \frac{1}{\xi}[\cos(h_1\xi)-\cos(h_2\xi)]\sin(z\xi)\,\mathrm{d}\xi\\
&A(\xi)\left[\varrho_5 I_0(R_o\xi\varrho_1) - (b-1)\frac{\varrho_1}{R_o\xi} I_1(R_o\xi\varrho_1)\right]\\
&+B(\xi)\left[\varrho_5 K_0(R_o\xi\varrho_1) + (b-1)\frac{\varrho_1}{R_o\xi} K_1(R_o\xi\varrho_1)\right]\\
&+C(\xi)\left[\varrho_6 I_0(R_o\xi\varrho_2) - (b-1)\frac{\varrho_2}{R_o\xi} I_1(R_o\xi\varrho_2)\right]\\
&+D(\xi)\left[\varrho_6 K_0(R_o\xi\varrho_2) + (b-1)\frac{\varrho_2}{R_o\xi} K_1(R_o\xi\varrho_2)\right]=0\\
&-\frac{2}{\pi}\int_0^\infty \xi[A(\xi)\varrho_1\varrho_5 I_1(R_o\xi\varrho_1) - B(\xi)\varrho_1\varrho_5 K_1(R_o\xi\varrho_1)\\
&+C(\xi)\varrho_2\varrho_6 I_1(R_o\xi\varrho_2) - D(\xi)\varrho_2\varrho_6 K_1(R_o\xi\varrho_2)]\sin(z\xi)\,\mathrm{d}\xi\\
&=\frac{2\tau_1}{\pi}\int_0^\infty \frac{1}{\xi}[\cos(h_3\xi)-\cos(h_4\xi)]\sin(z\xi)\,\mathrm{d}\xi
\end{aligned}
\tag{2}
$$

The above equations are rewritten to take the form

$$
\begin{aligned}
&A(\zeta)\Delta_{11}(\zeta)+B(\zeta)\Delta_{12}(\zeta)+C(\zeta)\Delta_{13}(\zeta)+D(\zeta)\Delta_{14}(\zeta)=0\\
&A(\zeta)\varrho_1\varrho_5 I_1(\zeta\varrho_1)-B(\zeta)\varrho_1\varrho_5 K_1(\zeta\varrho_1)+C(\zeta)\varrho_2\varrho_6 I_1(\zeta\varrho_2)-D(\zeta)\varrho_2\varrho_6 K_1(\zeta\varrho_2)\\
&\quad=\Sigma_1(\zeta)A(\zeta)\Delta_{11}(\alpha\zeta)+B(\zeta)\Delta_{12}(\alpha\zeta)+C(\zeta)\Delta_{13}(\alpha\zeta)+D(\zeta)\Delta_{14}(\alpha\zeta)=0\\
&A(\zeta)\varrho_1\varrho_5 I_1(\alpha\zeta\varrho_1)-B(\zeta)\varrho_1\varrho_5 K_1(\alpha\zeta\varrho_1)+C(\zeta)\varrho_2\varrho_6 I_1(\alpha\zeta\varrho_2)-D(\zeta)\varrho_2\varrho_6 K_1(\alpha\zeta\varrho_2)\\
&\quad=\Sigma_2(\zeta)
\end{aligned}
\tag{3}
$$

where in the above equations we have $\Sigma_1(\zeta)=\frac{\tau_2 R_i^2}{\zeta^2}\left[\cos\left(\frac{h_2}{R_i}\zeta\right)-\cos\left(\frac{h_1}{R_i}\zeta\right)\right]$ and $\Sigma_2(\zeta)=\frac{\tau_1 R_o^2}{(\alpha\zeta)^2}\left[\cos\left(\frac{h_4}{R_o}\alpha\zeta\right)-\cos\left(\frac{h_3}{R_o}\alpha\zeta\right)\right]=\frac{\tau_1 R_i^2}{\zeta^2}\left[\cos\left(\frac{h_4}{R_i}\zeta\right)-\cos\left(\frac{h_3}{R_i}\zeta\right)\right]$. Solution of Eq. (3) gives the coefficients of $A(\zeta), B(\zeta), C(\zeta)$, and $D(\zeta)$ which are similar to that given in Appendix B of part I of the paper, but the parameters $\Lambda_1(\zeta), \Lambda_2(\zeta), \Lambda_3(\zeta)$, and $\Lambda_4(\zeta)$ are replaced by $0, \Sigma_1(\zeta), 0$ and $\Sigma_2(\zeta)$, respectively, and we eliminate the multiplier $\frac{b_z R_i}{2\lambda}$ from the solution. Finally, the stress components are given by

$$
\begin{aligned}
\sigma_{rr}(r,z)=\frac{2}{\pi R_i^2}\int_0^\infty &\left\{A(\zeta)\left[\varrho_5\zeta I_0\left(\frac{r\varrho_1}{R_i}\zeta\right)-(b-1)R_i\varrho_1 I_1\left(\frac{r\varrho_1}{R_i}\zeta\right)/r\right]\right.\\
&+B(\zeta)\left[\varrho_5\zeta K_0\left(\frac{r\varrho_1}{R_i}\zeta\right)+(b-1)R_i\varrho_1 K_1\left(\frac{r\varrho_1}{R_i}\zeta\right)/r\right]\\
&\left.+C(\zeta)\left[\varrho_6\zeta I_0\left(\frac{r\varrho_2}{R_i}\zeta\right)-(b-1)R_i\varrho_2 I_1\left(\frac{r\varrho_2}{R_i}\zeta\right)/r\right]\right.
\end{aligned}
$$

$$+D(\zeta)\left[\varrho_6\zeta K_0\left(\frac{r\varrho_2}{R_i}\zeta\right)+(b-1)R_i\varrho_2K_1\left(\frac{r\varrho_2}{R_i}\zeta\right)/r\right]\Bigg\}\cos\left(z\frac{\zeta}{R_i}\right)\mathrm{d}\zeta$$

$$\sigma_{rz}(r,z)=-\frac{2}{\pi R_i^2}\int_0^\infty\zeta\left[A(\zeta)\varrho_1\varrho_5I_1\left(\frac{r\varrho_1}{R_i}\zeta\right)-B(\zeta)\varrho_1\varrho_5K_1\left(\frac{r\varrho_1}{R_i}\zeta\right)\right.$$
$$\left.+C(\zeta)\varrho_2\varrho_6I_1\left(\frac{r\varrho_2}{R_i}\zeta\right)-D(\zeta)\varrho_2\varrho_6K_1\left(\frac{r\varrho_2}{R_i}\zeta\right)\right]\sin\left(\frac{z}{R_i}\zeta\right)\mathrm{d}\zeta$$

$$\sigma_{zz}(r,z)=\frac{2}{\pi R_i^2}\int_0^\infty\zeta\left[A(\zeta)\varrho_7I_0\left(\frac{r\varrho_1}{R_i}\zeta\right)+B(\zeta)\varrho_7K_0\left(\frac{r\varrho_1}{R_i}\zeta\right)\right.$$
$$\left.+C(\zeta)\varrho_8I_0\left(\frac{r\varrho_2}{R_i}\zeta\right)+D(\zeta)\varrho_8K_0\left(\frac{r\varrho_2}{R_i}\zeta\right)\right]\cos\left(\frac{z}{R_i}\zeta\right)\mathrm{d}\zeta \tag{4}$$

2.2. Tension of an intact finite hollow cylinder under lateral shear tractions

We consider an intact finite hollow cylinder with height $2h$ and inner and outer radii R_i and R_o, respectively, Fig. 2, in which the flat surfaces of the cylinder, that is, $z=\pm h$ are stress-free. Also, the inner curved surface of the cylinder is left stress-free except for regions $h_1<z<h_2$ and $-h_2<z<-h_1$. Similarly, the outer lateral surface of the cylinder is kept stress-free except for regions $h_3<z<h_4$ and $-h_4<z<-h_3$. In the inner surface, the cylinder is under constant shear tractions τ_2 and $-\tau_2$ which are applied in the opposite directions. Analogously, the outer surface is subjected to constant shear tractions τ_1 and $-\tau_1$. In fact, the cylinder is subjected to two identical bidirectional tractions on each curved surface, which are applied near the two ends of cylinder in the opposite directions. The lateral boundary conditions of the problem are exactly the same as the intact infinite hollow cylinder, that is, Eq. (1). The upper and lower faces of the cylinder are stress-free. Therefore, the boundary conditions $\sigma_{pz}(r,\pm h)=0, p=r,z$ should be applied. The problem of an intact finite hollow cylinder is symmetric with respect to $z=0$. Therefore, solution to Eq. (5) of part I is given in the series form as [1]

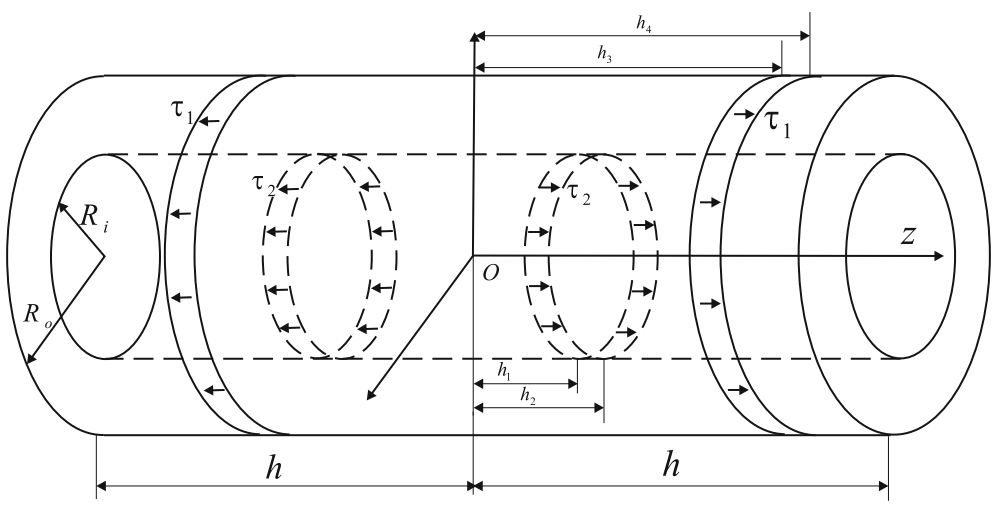

Fig. 2. A finite hollow cylinder under lateral constant bidirectional shear tractions

$$\chi(r,z)=\sum_{i=1}^{\infty}\frac{1}{\eta_i^3}\left[A_iI_0(\varrho_1\eta_ir)+B_iK_0(\varrho_1\eta_ir)+C_iI_0(\varrho_2\eta_ir)+D_iK_0(\varrho_2\eta_ir)\right]\sin(\eta_iz)$$
$$+\sum_{n=1}^{\infty}\frac{1}{\lambda_n^3}\left[E_n\sin h\left(\varrho_1\lambda_nz/\sqrt{f}\right)+F_n\sin h\left(\varrho_2\lambda_nz/\sqrt{f}\right)\right]\left[J_0(\lambda_nr)+T_nY_0(\lambda_nr)\right] \quad (5)$$

where $A_i, B_i, C_i, D_i, E_n, F_n$, and T_n are the unknown coefficients and $\eta_i = i\pi/h$ and λ_n are the roots of the equation $J_1(\lambda_nR_i)-\frac{J_1(\lambda_nR_o)}{Y_1(\lambda_nR_o)}Y_1(\lambda_nR_i)=0$. It is worth mentioning that $\lambda_1=0$ is the trivial root of this equation. Substituting Eq. (5) into relations (3) of part I, the stress components are derived as follows:

$$\sigma_{rr}(r,z)=\sum_{i=1}^{\infty}\left\{A_i\left[\varrho_5I_0(\varrho_1\eta_ir)-\frac{(b-1)\varrho_1}{\eta_ir}I_1(\varrho_1\eta_ir)\right]\right.$$
$$+B_i\left[\varrho_5K_0(\varrho_1\eta_ir)+\frac{(b-1)\varrho_1}{\eta_ir}K_1(\varrho_1\eta_ir)\right]$$
$$\left.+C_i\left[\varrho_6I_0(\varrho_2\eta_ir)-\frac{(b-1)\varrho_2}{\eta_ir}I_1(\varrho_2\eta_ir)\right]+D_i\left[\varrho_6K_0(\varrho_1\eta_ir)+\frac{(b-1)\varrho_2}{\eta_ir}K_1(\varrho_2\eta_ir)\right]\right\}$$
$$\cos(\eta_iz)+A_0\left[\varrho_5-\frac{(b-1)(\varrho_1)^2}{2}\right]+C_0\left[\varrho_6-\frac{(b-1)(\varrho_2)^2}{2}\right]+\frac{1}{\sqrt{f}}$$
$$\times\sum_{n=1}^{\infty}\left\{\varrho_1\left\{\frac{f-a\varrho_1^2}{f}\left[J_0(\lambda_nr)+T_nY_0(\lambda_nr)\right]+\frac{(b-1)}{r\lambda_n}\left[J_1(\lambda_nr)+T_nY_1(\lambda_nr)\right]\right\}\right.$$
$$E_n\cos h\left(\frac{\varrho_1\lambda_n}{\sqrt{f}}z\right)+\varrho_2\left\{\frac{f-a\varrho_2^2}{f}\left[J_0(\lambda_nr)+T_nY_0(\lambda_nr)\right]\right.$$
$$\left.\left.+\frac{(b-1)}{r\lambda_n}\left[J_1(\lambda_nr)+T_nY_1(\lambda_nr)\right]\right\}F_n\cos h\left(\frac{\varrho_2\lambda_n}{\sqrt{f}}z\right)\right\}$$
$$\sigma_{rz}(r,z)=-\sum_{i=1}^{\infty}\left\{\varrho_1\varrho_5\left[A_iI_1(\varrho_1\eta_ir)-B_iK_1(\varrho_1\eta_ir)\right]\right.$$
$$\left.+\varrho_2\varrho_6\left[C_iI_1(\varrho_2\eta_ir)-D_iK_1(\varrho_2\eta_ir)\right]\right\}\sin(\eta_iz)$$
$$+\frac{1}{f}\sum_{n=1}^{\infty}\left[\left(f-a\varrho_1^2\right)E_n\sin h\left(\frac{\varrho_1\lambda_n}{\sqrt{f}}z\right)+\left(f-a\varrho_2^2\right)F_n\sin h\left(\frac{\varrho_2\lambda_n}{\sqrt{f}}z\right)\right]\left[J_1(\lambda_nr)+T_nY_1(\lambda_nr)\right]$$
$$\sigma_{zz}(r,z)=A_0\varrho_7+\varrho_8C_0$$
$$+\sum_{i=1}^{\infty}\left\{\varrho_7\left[A_iI_0(\varrho_1\eta_ir)+B_iK_0(\varrho_1\eta_ir)\right]+\varrho_8\left[C_iI_0(\varrho_2\eta_ir)+D_iK_0(\varrho_2\eta_ir)\right]\right\}\cos(\eta_iz)$$
$$+\frac{1}{\sqrt{f}}\sum_{n=1}^{\infty}\left\{\varrho_1\left(\varrho_1^2-c\right)E_n\cos h\left(\frac{\varrho_1\lambda_n}{\sqrt{f}}z\right)\right.$$
$$\left.+\varrho_2\left(\varrho_2^2-c\right)F_n\cos h\left(\frac{\varrho_2\lambda_n}{\sqrt{f}}z\right)\right\}\left[J_0(\lambda_nr)+T_nY_0(\lambda_nr)\right] \quad (6)$$

The terms with coefficients A_0, C_0 are coming from $i=0$ for cosine series including the term $\cos(\eta_iz)$. By choosing $T_n=-\frac{J_1(\lambda_nR_i)}{Y_1(\lambda_nR_i)}=-\frac{J_1(\lambda_nR_o)}{Y_1(\lambda_nR_o)}$ and making use of the Fourier sine series of the Heaviside step function, i.e., the series $H(z-h_k)=\frac{2}{h}\sum_{i=1}^{\infty}\frac{1}{\eta_i}\cos(\eta_ih_k)\sin(\eta_iz), k=1,2,3,4$. The boundary conditions (1) and $\sigma_{rz}(r,h)=0$ are applied, giving

$$
\begin{aligned}
&A_0\left[\varrho_5-\frac{(b-1)\left(\varrho_1\right)^2}{2}\right]+C_0\left[\varrho_6-\frac{(b-1)\left(\varrho_2\right)^2}{2}\right]=0\\
&A_i\Pi_2\left(\eta_i R_i,\varrho_1,\varrho_5\right)+B_i\Pi_3\left(\eta_i R_i,\varrho_1,\varrho_5\right)+C_i\Pi_2\left(\eta_i R_i,\varrho_2,\varrho_6\right)+D_i\Pi_3\left(\eta_i R_i,\varrho_2,\varrho_6\right)\\
&\quad=\sum_{n=1}^{\infty}\Pi_1\left(\varrho_1/\sqrt{f},R_i,\eta_i,\lambda_n\right)E_n+\Pi_1\left(\varrho_2/\sqrt{f},R_i,\eta_i,\lambda_n\right)F_n, i=0,1,2,\ldots\\
&A_i\Pi_2\left(\eta_i R_o,\varrho_1,\varrho_5\right)+B_i\Pi_3\left(\eta_i R_o,\varrho_1,\varrho_5\right)+C_i\Pi_2\left(\eta_i R_o,\varrho_2,\varrho_6\right)+D_i\Pi_3\left(\eta_i R_o,\varrho_2,\varrho_6\right)\\
&\quad=\sum_{n=1}^{\infty}\Pi_1\left(\varrho_1/\sqrt{f},R_o,\eta_i,\lambda_n\right)E_n+\Pi_1\left(\varrho_2/\sqrt{f},R_o,\eta_i,\lambda_n\right)F_n, i=0,1,2,\ldots\\
&\varrho_1\varrho_5\left[A_iI_1\left(\varrho_1\eta_iR_i\right)-B_iK_1\left(\varrho_1\eta_iR_i\right)\right]+\varrho_2\varrho_6\left[C_iI_1\left(\varrho_2\eta_iR_i\right)-D_iK_1\left(\varrho_2\eta_iR_i\right)\right]\\
&\quad=-\frac{2\tau_2}{h\eta_i}\left[\cos\left(\eta_ih_1\right)-\cos\left(\eta_ih_2\right)\right],\quad i=1,2,\ldots\\
&\varrho_1\varrho_5\left[A_iI_1\left(\varrho_1\eta_iR_o\right)-B_iK_1\left(\varrho_1\eta_iR_o\right)\right]+\varrho_2\varrho_6\left[C_iI_1\left(\varrho_2\eta_iR_o\right)-D_iK_1\left(\varrho_2\eta_iR_o\right)\right]\\
&\quad=-\frac{2\tau_1}{h\eta_i}\left[\cos\left(\eta_ih_3\right)-\cos\left(\eta_ih_4\right)\right],\quad i=1,2,\ldots\\
&\left(f-a\varrho_1^2\right)E_n\sin h\left(\frac{\varrho_1\lambda_n}{\sqrt{f}}h\right)+\left(f-a\varrho_2^2\right)F_n\sin h\left(\frac{\varrho_2\lambda_n}{\sqrt{f}}h\right)=0
\end{aligned}
\tag{7}
$$

where

$$
\begin{aligned}
&\Pi_1\left(x,y,\eta_i,\lambda_n\right)=-\frac{2\left(-1\right)^i x^2\left(1-ax^2\right)\lambda_n\sin h\left(x\lambda_nh\right)Z\left(\lambda_ny\right)}{h\left[\left(x\lambda_n\right)^2+\eta_i^2\right]}\\
&\Pi_2\left(x,y,t\right)=tI_0\left(xy\right)-\frac{(b-1)\,y}{x}I_1\left(xy\right),\Pi_3\left(x,y,t\right)=tK_0\left(xy\right)+\frac{(b-1)\,y}{x}K_1\left(xy\right)
\end{aligned}
\tag{8}
$$

in which δ_{i0} is Kronecker delta and $Z\left(\lambda_ny\right)=J_0\left(\lambda_ny\right)-\frac{J_1(\lambda_nR_i)}{Y_1(\lambda_nR_i)}Y_0\left(\lambda_ny\right)$. Using the last equation of (7) the coefficients $\Pi_1\left(\varrho_1/\sqrt{f},R_j,\eta_i,\lambda_n\right)E_n+\Pi_1\left(\varrho_2/\sqrt{f},R_j,\eta_i,\lambda_n\right)F_n, j=i,O$ are simplified to $\frac{2(-1)^{i+1}\left(f-a\varrho_1^2\right)\left(\left(\varrho_1\right)^2-\left(\varrho_2\right)^2\right)\lambda_n\sin h\left(\frac{\varrho_1\lambda_n}{\sqrt{f}}h\right)\eta_i^2Z(\lambda_nR_j)}{hf^2\left[\left(\frac{\varrho_1\lambda_n}{\sqrt{f}}\right)^2+\eta_i^2\right]\left[\left(\frac{\varrho_2\lambda_n}{\sqrt{f}}\right)^2+\eta_i^2\right]}E_n$. Applying the remainder boundary condition, i.e., $\sigma_{zz}\left(r,h\right)=0$, by virtue of the last equation of (7), leads to

$$
\begin{aligned}
&A_0\varrho_7+\varrho_8C_0+\sum_{i=1}^{\infty}\left\{\varrho_7\left[A_iI_0\left(\varrho_1\eta_ir\right)+B_iK_0\left(\varrho_1\eta_ir\right)\right]\right.\\
&\left.+\varrho_8\left[C_iI_0\left(\varrho_2\eta_ir\right)+D_iK_0\left(\varrho_2\eta_ir\right)\right]\right\}\left(-1\right)^i=-\frac{1}{\sqrt{f}}\sum_{n=1}^{\infty}\left\{\varrho_1\left(\varrho_1^2-c\right)\cos h\left(\frac{\varrho_1\lambda_n}{\sqrt{f}}h\right)\right.\\
&\left.-\varrho_2\left(\varrho_2^2-c\right)\frac{\left(f-a\varrho_1^2\right)}{\left(f-a\varrho_2^2\right)}\sin h\left(\frac{\varrho_1\lambda_n}{\sqrt{f}}h\right)\cot h\left(\frac{\varrho_2\lambda_n}{\sqrt{f}}h\right)\right\}Z\left(\lambda_nr\right)E_n
\end{aligned}
\tag{9}
$$

The Fourier–Bessel's series of the function $f\left(r\right)$ in terms of the eigenfunctions $Z\left(\lambda_nr\right)$ is $f\left(r\right)=\sum_{n=1}^{\infty}A_nZ\left(\lambda_nr\right)$ in which $A_n=\frac{1}{Z(\lambda_nr)^2}\int_{R_i}^{R_o}rf\left(r\right)Z\left(\lambda_nr\right)\mathrm{d}r$ and $Z\left(\lambda_nr\right)$ is the norm of the eigenfunctions. Therefore, Eq. (9) is rewritten as follows

$$E_n = \omega_n \left\{ \left(A_0\varrho_7 + \varrho_8 C_0\right) \int_{R_i}^{R_o} rZ\left(\lambda_n r\right) \mathrm{d}r \right.$$
$$+ \sum_{i=1}^{\infty} \left\{ \varrho_7 \left[A_i \int_{R_i}^{R_o} rI_0\left(\varrho_1\eta_i r\right) Z\left(\lambda_n r\right) \mathrm{d}r + B_i \int_{R_i}^{R_o} rK_0\left(\varrho_1\eta_i r\right) Z\left(\lambda_n r\right) \mathrm{d}r \right] \right.$$
$$\left. \left. \varrho_8 \left[C_i \int_{R_i}^{R_o} rI_0\left(\varrho_2\eta_i r\right) Z\left(\lambda_n r\right) \mathrm{d}r + D_i \int_{R_i}^{R_o} rK_0\left(\varrho_2\eta_i r\right) Z\left(\lambda_n r\right) \mathrm{d}r \right] \right\} \left(-1\right)^i \right\} \tag{10}$$

in which ω_n and $Z\left(\lambda_n r\right) = \left\{ \int_{R_i}^{R_o} r\left[Z\left(\lambda_n r\right)\right]^2 \mathrm{d}r \right\}^{\frac{1}{2}}$ are as follows

$$Z\left(\lambda_n r\right) = \left\{ \frac{1}{2}\left(R_o\right)^2 \left[J_0\left(\lambda_n R_o\right) - \frac{J_1\left(\lambda_n R_i\right)}{Y_1\left(\lambda_n R_i\right)} Y_0\left(\lambda_n R_o\right) \right]^2 - \frac{2}{\left(\pi\lambda_n Y_1\left(\lambda_n R_i\right)\right)^2} \right\}^{\frac{1}{2}}$$
$$\omega_n = \frac{-\sqrt{f}\sin h\left(\frac{\varrho_1\lambda_n}{\sqrt{f}}h\right)}{Z\left(\lambda_n r\right)^2 \left\{ \varrho_1\left(\varrho_1^2 - c\right)\cot h\left(\frac{\varrho_1\lambda_n}{\sqrt{f}}h\right) - \varrho_2\left(\varrho_2^2 - c\right)\frac{\left(f - a\varrho_1^2\right)}{\left(f - a\varrho_2^2\right)}\cot h\left(\frac{\varrho_2\lambda_n}{\sqrt{f}}h\right) \right\}} \tag{11}$$

Also we arrive at $A_0\varrho_7 + \varrho_8 C_0 = 0$. Therefore, viewing the first equation of (7) we conclude that $A_0 = C_0 = 0$. Evaluating the integrals in Eq. (10) can be downed by relations given in Appendix A of this part as

$$E_n = \omega_n \left\{ \sum_{i=1}^{\infty} \left\{ \varrho_7 \{ A_i \left[\varpi_1\left(\varrho_1\eta_i, \lambda_n\right) - \varpi_2\left(\varrho_1\eta_i, \lambda_n\right) \frac{J_1\left(\lambda_n R_i\right)}{Y_1\left(\lambda_n R_i\right)} \right] \right.\right.$$
$$\left. + B_i \left[\varpi_3\left(\varrho_1\eta_i, \lambda_n\right) - \varpi_4\left(\varrho_1\eta_i, \lambda_n\right) \frac{J_1\left(\lambda_n R_i\right)}{Y_1\left(\lambda_n R_i\right)} \right] \right\}$$
$$+ \varrho_8 \left\{ C_i \left[\varpi_1\left(\varrho_2\eta_i, \lambda_n\right) - \varpi_2\left(\varrho_2\eta_i, \lambda_n\right) \frac{J_1\left(\lambda_n R_i\right)}{Y_1\left(\lambda_n R_i\right)} \right] \right.$$
$$\left. \left. + D_i \left[\varpi_3\left(\varrho_2\eta_i, \lambda_n\right) - \varpi_4\left(\varrho_2\eta_i, \lambda_n\right) \frac{J_1\left(\lambda_n R_i\right)}{Y_1\left(\lambda_n R_i\right)} \right] \right\} \left(-1\right)^i \right\} \tag{12}$$

Substituting E_n from the above equation into the last equation of (7) and substituting the ensuing equations into the first equations of (7) yields

$$A_i\Pi_2\left(\eta_i R_i, \varrho_1, \varrho_5\right) + B_i\Pi_3\left(\eta_i R_i, \varrho_1, \varrho_5\right) + C_i\Pi_2\left(\eta_i R_i, \varrho_2, \varrho_6\right) + D_i\Pi_3\left(\eta_i R_i, \varrho_2, \varrho_6\right)$$
$$= \frac{2\left(-1\right)^{i+1}\left(f - a\varrho_1^2\right)\left(\left(\varrho_1\right)^2 - \left(\varrho_2\right)^2\right)\eta_i^2}{hf^2} \sum_{n=1}^{\infty} \frac{\lambda_n \sin h\left(\frac{\varrho_1\lambda_n}{\sqrt{f}}h\right) Z\left(\lambda_n R_i\right)\omega_n}{\left[\left(\frac{\varrho_1\lambda_n}{\sqrt{f}}\right)^2 + \eta_i^2\right]\left[\left(\frac{\varrho_2\lambda_n}{\sqrt{f}}\right)^2 + \eta_i^2\right]}$$
$$\left\{ \sum_{j=1}^{\infty} \left\{ \varrho_7 \{ A_j \left[\varpi_1\left(\varrho_1\eta_j, \lambda_n\right) - \varpi_2\left(\varrho_1\eta_j, \lambda_n\right) \frac{J_1\left(\lambda_n R_i\right)}{Y_1\left(\lambda_n R_i\right)} \right] \right.\right.$$
$$\left. + B_j \left[\varpi_3\left(\varrho_1\eta_j, \lambda_n\right) - \varpi_4\left(\varrho_1\eta_j, \lambda_n\right) \frac{J_1\left(\lambda_n R_i\right)}{Y_1\left(\lambda_n R_i\right)} \right] \right\}$$

$$
\begin{aligned}
&+\varrho_8\left\{C_j\left[\varpi_1\left(\varrho_2\eta_j,\lambda_n\right)-\varpi_2\left(\varrho_2\eta_j,\lambda_n\right)\frac{J_1\left(\lambda_nR_i\right)}{Y_1\left(\lambda_nR_i\right)}\right]\right.\\
&\left.+D_j\left[\varpi_3\left(\varrho_2\eta_j,\lambda_n\right)-\varpi_4\left(\varrho_2\eta_j,\lambda_n\right)\frac{J_1\left(\lambda_nR_i\right)}{Y_1\left(\lambda_nR_i\right)}\right]\right\}(-1)^j\Bigg\},\quad i=0,1,2,\ldots\\
&A_i\Pi_2\left(\eta_iR_o,\varrho_1,\varrho_5\right)+B_i\Pi_3\left(\eta_iR_o,\varrho_1,\varrho_5\right)+C_i\Pi_2\left(\eta_iR_o,\varrho_2,\varrho_6\right)+D_i\Pi_3\left(\eta_iR_o,\varrho_2,\varrho_6\right)\\
&=\frac{2(-1)^{i+1}\left(f-a\varrho_1^2\right)\left(\left(\varrho_1\right)^2-\left(\varrho_2\right)^2\right)\eta_i^2}{hf^2}\sum_{n=1}^{\infty}\frac{\lambda_n\sin h\left(\frac{\varrho_1\lambda_n}{\sqrt{f}}h\right)Z\left(\lambda_nR_o\right)\omega_n}{\left[\left(\frac{\varrho_1\lambda_n}{\sqrt{f}}\right)^2+\eta_i^2\right]\left[\left(\frac{\varrho_2\lambda_n}{\sqrt{f}}\right)^2+\eta_i^2\right]}\\
&\left\{\sum_{j=1}^{\infty}\left\{\varrho_7\{A_j\left[\varpi_1\left(\varrho_1\eta_j,\lambda_n\right)-\varpi_2\left(\varrho_1\eta_j,\lambda_n\right)\frac{J_1\left(\lambda_nR_i\right)}{Y_1\left(\lambda_nR_i\right)}\right]\right.\right.\\
&\left.+B_j\left[\varpi_3\left(\varrho_1\eta_j,\lambda_n\right)-\varpi_4\left(\varrho_1\eta_j,\lambda_n\right)\frac{J_1\left(\lambda_nR_i\right)}{Y_1\left(\lambda_nR_i\right)}\right]\right\}\\
&+\varrho_8\left\{C_j\left[\varpi_1\left(\varrho_2\eta_j,\lambda_n\right)-\varpi_2\left(\varrho_2\eta_j,\lambda_n\right)\frac{J_1\left(\lambda_nR_i\right)}{Y_1\left(\lambda_nR_i\right)}\right]\right.\\
&\left.\left.+D_j\left[\varpi_3\left(\varrho_2\eta_j,\lambda_n\right)-\varpi_4\left(\varrho_2\eta_j,\lambda_n\right)\frac{J_1\left(\lambda_nR_i\right)}{Y_1\left(\lambda_nR_i\right)}\right]\right\}(-1)^j\right\},\quad i=0,1,2,\ldots
\end{aligned}
\tag{13}
$$

The truncated form (the infinite series are truncated with N terms) of the above equations in association with the third and fourth equation of (7) constructs a system of $4N\times 4N$ algebraic equations in terms of the unknowns $\{A_i,B_i,C_i,D_i,i=1,2,\ldots,N\}$.

3. A finite hollow cylinder with multiple axisymmetric cracks: cutting method

Stress analysis of a finite hollow cylinder with some axisymmetric planar cracks can be followed by one of the following methods:

1. It is possible to solve the dislocation problem in a finite hollow cylinder. Next, using this solution, the problem of a cracked finite cylinder can also be solved. This is beyond the scope of this paper because the dislocation solution in the finite domains should be in the complicated series form. As it can be seen, the series solution obtained in Sect. 2.2 for tension analysis of an intact finite hollow cylinder is complex enough that we cannot simply extend it for a finite hollow cylinder with dislocation. In fact, we need an additional dislocation solution besides that accomplished at part I.
2. It is possible to consider an equivalent infinite hollow cylinder with two additional annular cracks besides the existing cracks of the finite hollow cylinder. In this case, the infinite hollow cylinder can be cut by extension of these two annular cracks and it can be changed to a finite hollow cylinder (we named it "cutting method"), Fig. 3. Validity of such a cutting method is shown in the following.

In this study, we pursue the second method [2]. We consider a finite hollow cylinder with length $2h$ which is subjected to two self-equilibrating distributed tractions, Fig. 2. One of these distributed tractions is defined by Eq. (1), and the other one is its image with respect to the middle plane of the cylinder ($z=0$). The stress field of an intact infinite hollow cylinder (Eq. 4) and an intact finite hollow cylinder (Eq. 6) can be compared for a short finite cylinder (for example, $h=1.5R_i$ and $R_i=0.5R_o$) in Figs. 4, 5 and 6 (for some sample values of z). Also we set $h_1=h_3=0.8R_i$ and $h_2=h_4=R_i$ as well as $\tau_1=\tau_2=\tau_0$. The cylinder is made of the magnesium whose material properties are chosen from Table 1. As we expect for short cylinders these stress fields must be different. Figures 4, 5, and 6 show

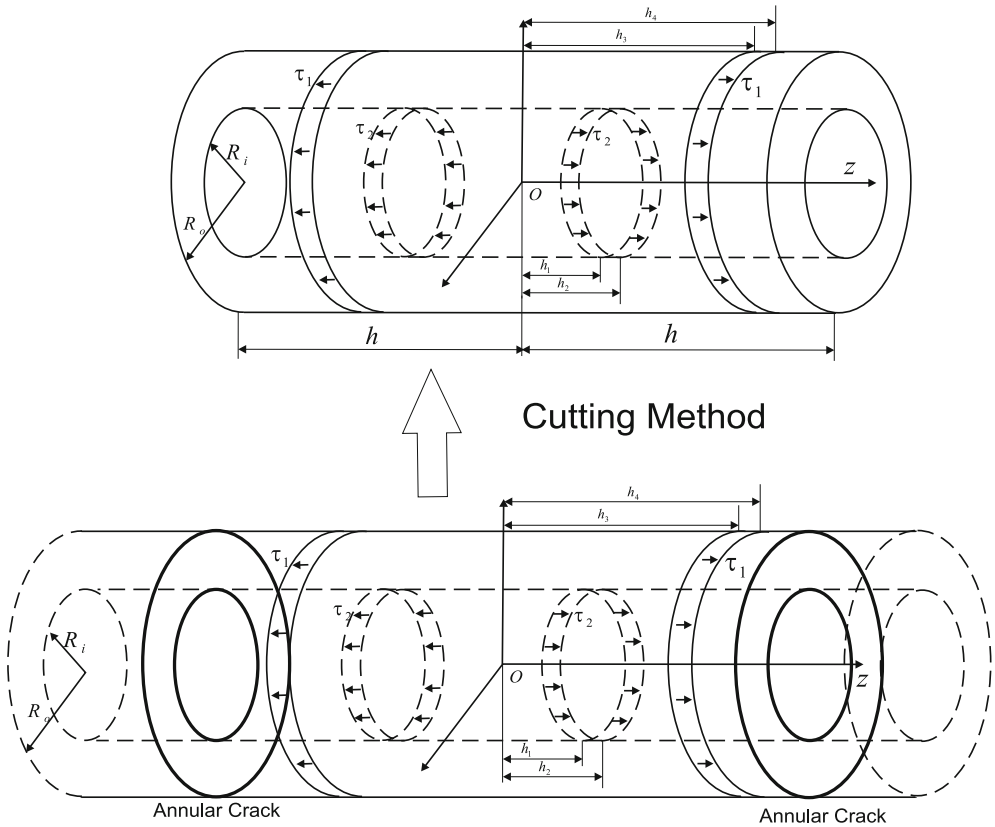

FIG. 3. The configuration describing the cutting method

the considerable discrepancies between the values of the stress components of the infinite and those of the finite hollow cylinders. In order to apply the "cutting method," we consider an infinite hollow cylinder by two annular axisymmetric cracks located at $z = \pm h$. The inner radii of these cracks are condensed to the inner radius of hollow cylinder, and the outer radii of them are extended to the outer radius of the cylinder. Consequently, a finite cylinder is obtained provided that an identical loading between $-h \leq z \leq h$ to be applied on both infinite and finite cylinders. To show the validity of such a method, we distribute four dislocations with densities $b_{z1}(t), b_{z2}(t), b_{r1}(t)$ and $b_{r2}(t)$ on the surfaces of two annular axisymmetric cracks. These cracks are located at $z_1 = h$ and $z_2 = -h$ of an infinite hollow cylinder, respectively.

Using Eqs. (19) and (25) of part I of the paper, the stress field emanating of these dislocation distributions is given by replacing ε with $r_j(t)$ and z with $|z - z_j|$ where $r_j(t) = 0.5[(R_o - R_i)t + (R_o + R_i)]$ and $L_j = 0.5(R_o - R_i), j = 1, 2$. Also according to the remark noted before (we mean part I), the term $\operatorname{sgn}(z - z_j)$ is multiplied to the relevant stress component whenever needed. By setting $r = r_i(s) = 0.5[(R_o - R_i)s + (R_o + R_i)], i = 1, 2, -1 \leq s \leq 1$ in Eqs. (19) and (25) of part I of the paper and considering the closure equation, i.e., $\int_{-1}^{1} b_{zj}(t)\,dt = 0$, $\int_{-1}^{1} b_{rj}(t)\,dt = 0, j = 1, 2$ two integral equations are derived. They are used to calculate the dislocation density functions $b_{z1}(t), b_{z2}(t), b_{r1}(t)$, and $b_{r2}(t)$. The left-hand side of the above-mentioned equations, i.e., the stress components $\sigma_{rz}(r_i(s), z_i)$ and $\sigma_{zz}(r_i(s), z_i)$, is given by [see Eq. (4)]. For the case $\tau_1 = \tau_2 = \tau_0$, by virtue of Buckner's principle [3], the total the stress component $\sigma_{rz}(r, z)$ in the remainder slice of infinite cylinder, which in now a finite cylinder, is given, for example, as follows

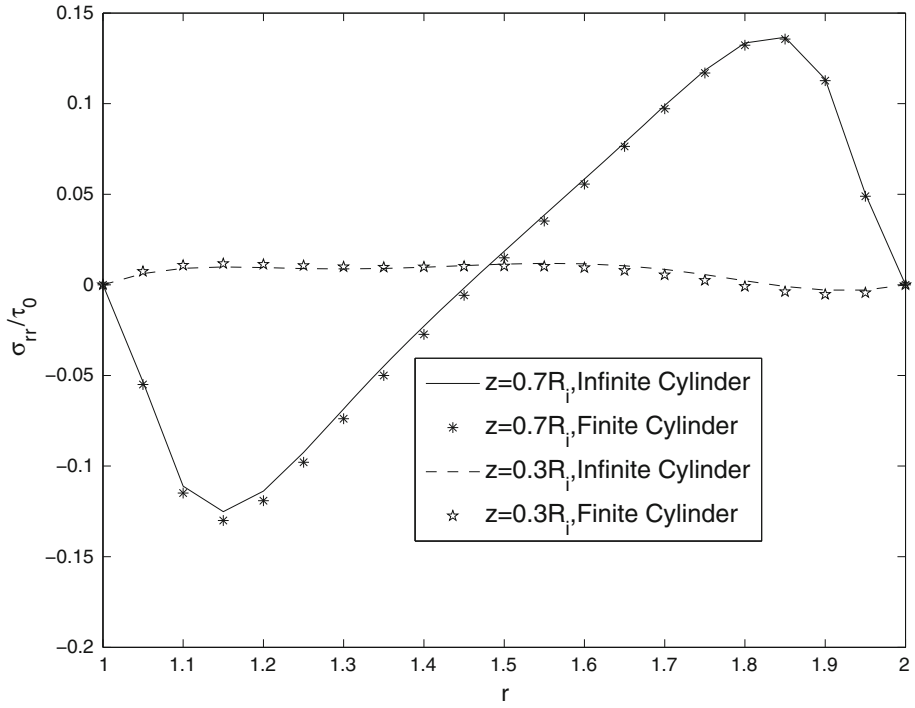

FIG. 4. The graph of the stress component $\sigma_{rr}(r,z)/\tau_0$ versus r obtained by Eqs. (4) and (6)

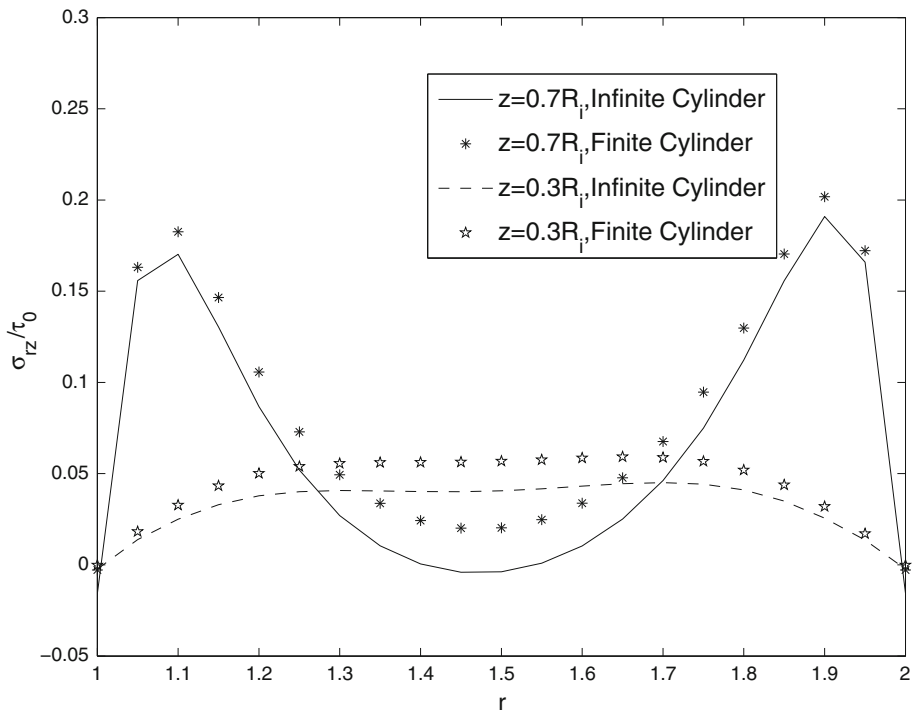

FIG. 5. The graph of the stress component $\sigma_{rz}(r,z)/\tau_0$ versus r obtained by Eqs. (4) and (6)

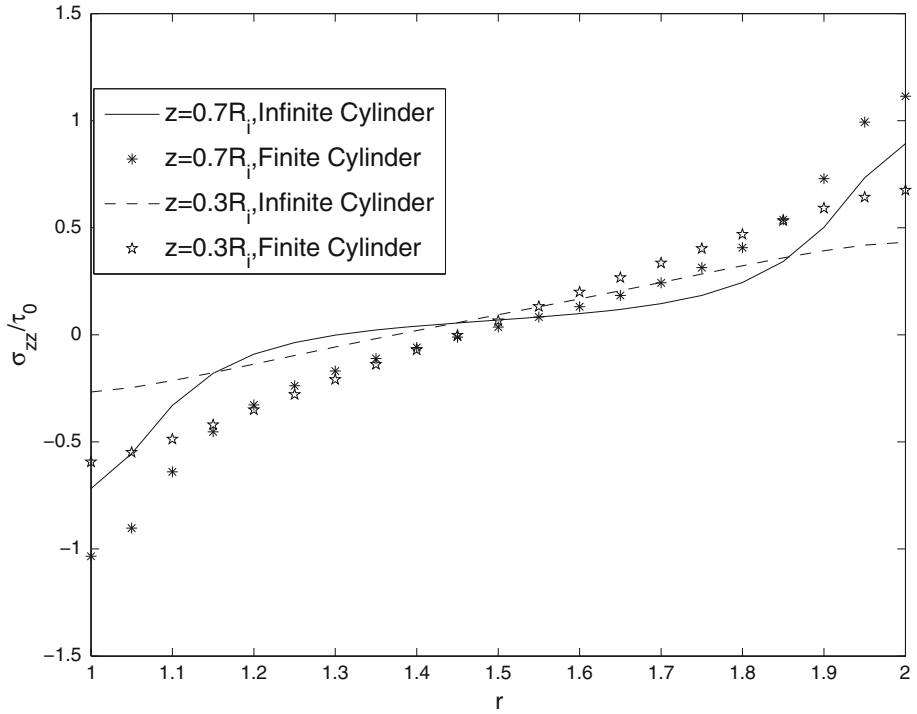

FIG. 6. The graph of the stress component $\sigma_{zz}(r,z)/\tau_0$ versus r obtained by Eqs. (4) and (6)

$$\sigma_{rz}(r,z) = -\frac{2\tau_0}{\pi R_i^2}\int_0^\infty \zeta\left[A_e(\zeta)\varrho_1\varrho_5 I_1\left(\frac{r\varrho_1}{R_i}\zeta\right) - B_e(\zeta)\varrho_1\varrho_5 K_1\left(\frac{r\varrho_1}{R_i}\zeta\right)\right.$$
$$\left. + C_e(\zeta)\varrho_2\varrho_6 I_1\left(\frac{r\varrho_2}{R_i}\zeta\right) - D_e(\zeta)\varrho_2\varrho_6 K_1\left(\frac{r\varrho_2}{R_i}\zeta\right)\right]\sin\left(\frac{z-z_j}{R_i}\zeta\right)\mathrm{d}\zeta - \frac{2}{\pi R_i^2}\mathrm{sgn}(z-z_j)$$
$$\sum_{j=1}^{2} L_j\int_{-1}^{1} b_{zj}(t)\left\{\int_0^\infty \zeta\left[A_c(\zeta,r_j(t))\varrho_1\varrho_5 I_1\left(\frac{r\varrho_1}{R_i}\zeta\right) - B_c(\zeta,r_j(t))\varrho_1\varrho_5 K_1\left(\frac{r\varrho_1}{R_i}\zeta\right)\right.\right.$$
$$\left.\left. + C_c(\zeta,r_j(t))\varrho_2\varrho_6 I_1\left(\frac{r\varrho_2}{R_i}\zeta\right) - D_c(\zeta,r_j(t))\varrho_2\varrho_6 K_1\left(\frac{r\varrho_2}{R_i}\zeta\right)\right]\sin\left(\frac{(z-z_j)}{R_i}\zeta\right)\mathrm{d}\zeta\right\}\mathrm{d}t$$
$$-\frac{\varrho_5\varrho_6}{2\lambda}\mathrm{sgn}(z-z_j)\sum_{j=1}^{2} L_j\int_{-1}^{1} b_{zj}(t)$$
$$\left\{\int_0^\infty\left[\mathrm{e}^{-\frac{\varrho_2\eta|z-z_j|}{\sqrt{f}}} - \mathrm{e}^{-\frac{\varrho_1\eta|z-z_j|}{\sqrt{f}}}\right][R_o J_1(\eta R_o) - r_j(t)J_1(r_j(t)\eta)]\eta J_1(r\eta)\,\mathrm{d}\eta\right\}\mathrm{d}t$$
$$-\frac{2}{\pi R_i^2}\sum_{j=1}^{2} L_j\int_{-1}^{1} b_{rj}(t)\left\{\int_0^\infty \zeta[A_g(\zeta,R_i)\varrho_1\varrho_5 I_1\left(\frac{r\varrho_1}{R_i}\zeta\right) - B_g(\zeta,R_i)\varrho_1\varrho_5 K_1\left(\frac{r\varrho_1}{R_i}\zeta\right)\right.$$

$$+ C_g(\zeta, R_i)\,\varrho_2\varrho_6 I_1\left(\frac{r\varrho_2}{R_i}\zeta\right) - D_g(\zeta, R_i)\,\varrho_2\varrho_6 K_1\left(\frac{r\varrho_2}{R_i}\zeta\right)]\cos\left((z-z_j)\,\xi\right)\mathrm{d}\zeta\Bigg\}\mathrm{d}t$$

$$-\frac{b_r}{2\kappa f R_i^2}\sum_{j=1}^{2} L_j \int_{-1}^{1} b_{rj}(t)$$

$$\left\{\int_0^{\infty}\eta^2\int_{r_j(t)/R_i}^{\alpha}\rho I_1(\rho\eta)\,\mathrm{d}\rho\left(\varrho_7\varrho_6\varrho_2 \mathrm{e}^{-\frac{\varrho_1\eta|z-z_j|}{\sqrt{f}}} - \varrho_8\varrho_5\varrho_1 \mathrm{e}^{-\frac{\varrho_2\eta|z-z_j|}{\sqrt{f}}}\right) J_1(r\eta)\,\mathrm{d}\eta\right\}\mathrm{d}t \qquad (14)$$

where the coefficients $A_e(\zeta),\ldots,D_e(\zeta)$ are obtained from Eq. (3) by eliminating the multiplier τ_0 from the coefficients $A(\zeta),\ldots,D(\zeta)$. Similarly, the coefficients $A_c(\zeta, r_j(t)),\ldots,D_c(\zeta, r_j(t))$ and $A_g(\zeta, r_j(t)),\ldots,D_g(\zeta, r_j(t))$ are obtained from the relations (17) and (27) of part I, respectively, in which the multipliers b_{zj} and b_{rj} are eliminated. Substituting $b_{z1}(t), b_{z2}(t), b_{r1}(t)$, and $b_{r2}(t)$, obtained by solving the relevant integral equations, into the above stress component leads to that of a finite hollow cylinder under the previously mentioned loading. Similarly, the total stress component $\sigma_{zz}(r,z)$ can be derived (for the sake of simplicity, we did not write it here). The graphs of the stress components $\sigma_{rr}(r,z)/\tau_0, \sigma_{rz}(r,z)/\tau_0$ and $\sigma_{zz}(r,z)/\tau_0$versus r and those obtained via Eq. (6) are shown in Figs. 7, 8, and 9. Comparison of the results verifies the cutting method.

4. Numerical examples and discussion

In this section, we provide some numerical examples to show the capabilities of the developed procedure in this article based on distributed dislocation technique to treat the problem of cracked finite hollow

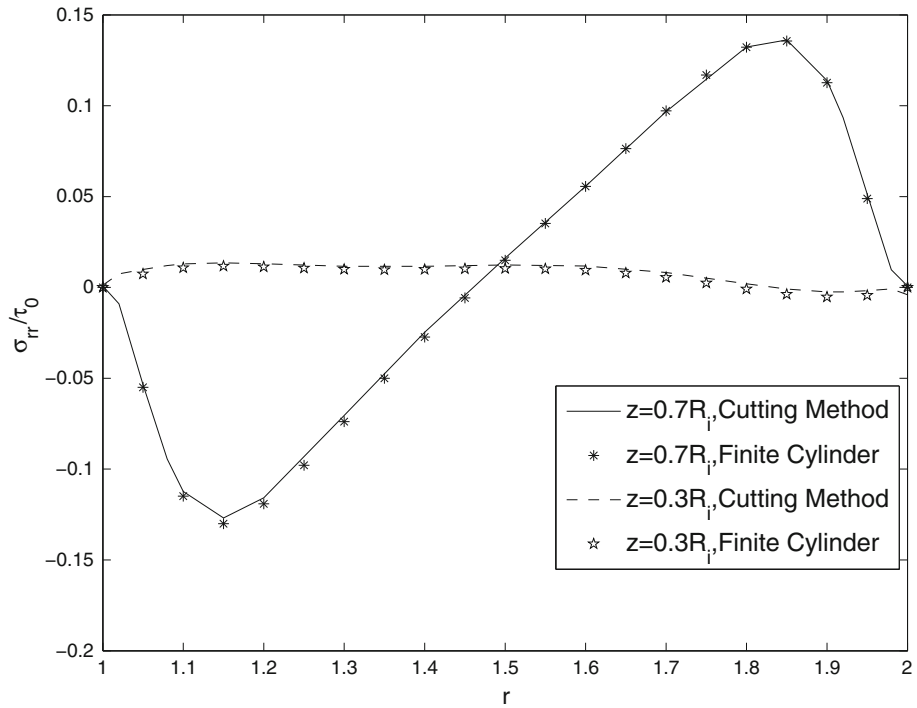

FIG. 7. The graph of the stress component $\sigma_{rr}(r,z)/\tau_0$ versus r obtained by Eqs. (14) and (6)

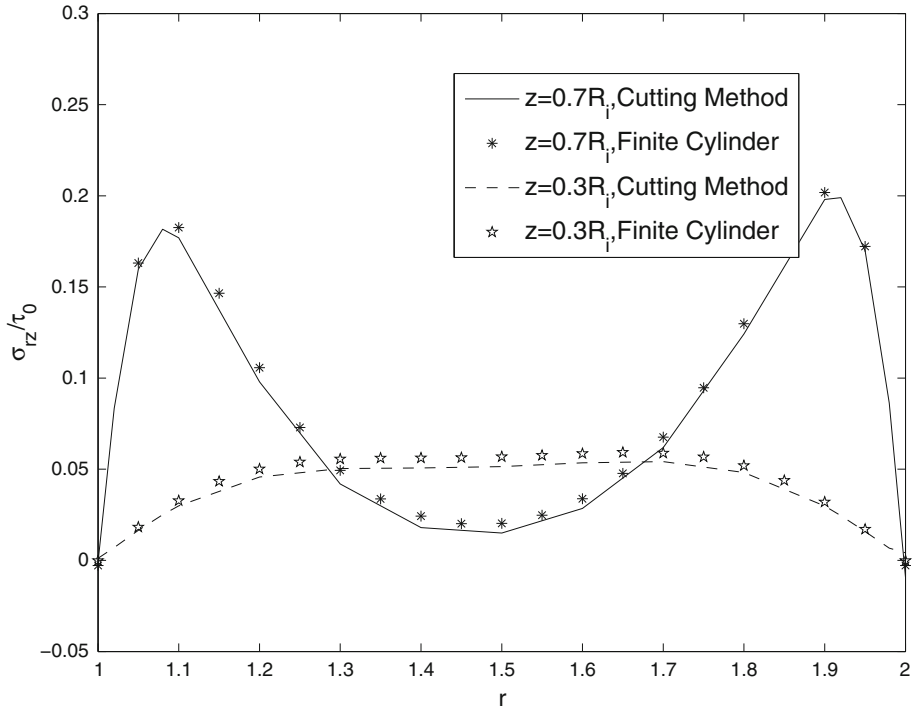

FIG. 8. The graph of the stress component $\sigma_{rz}(r,z)/\tau_0$ versus r obtained by Eqs. (14) and (6)

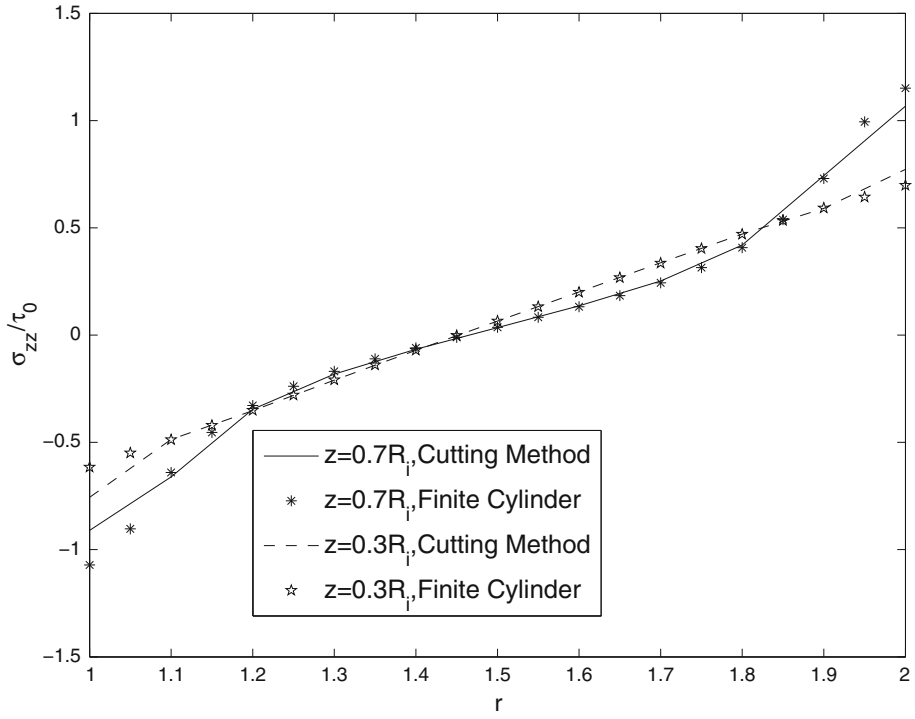

FIG. 9. The graph of the stress component $\sigma_{zz}(r,z)/\tau_0$ versus r obtained by Eqs. (14) and (6)

TABLE 1. *Normalized stress intensity factors for an annular crack of the hollow finite cylinder* ($R_o = 2R_i, h = 1.5R_i$)

Magnesium				
$r_i = 1.2R_i$	k_{IL}/k_0	0.0137	k_{IIL}/k_0	0.0109
$r_f = 1.8R_i$	k_{IR}/k_0	0.0487	k_{IIR}/k_0	0.0140
$r_i = 1.1R_i$	k_{IL}/k_0	0.0434	k_{IIL}/k_0	0.0378
$r_f = 1.9R_i$	k_{IR}/k_0	0.1055	k_{IIR}/k_0	0.0401
Cadmium				
$r_i = 1.2R_i$	k_{IL}/k_0	0.003	k_{IIL}/k_0	0.0188
$r_f = 1.8R_i$	k_{IR}/k_0	0.0477	k_{IIR}/k_0	0.0199
$r_i = 1.1R_i$	k_{IL}/k_0	0.0241	k_{IIL}/k_0	0.0412
$r_f = 1.9R_i$	k_{IR}/k_0	0.103	k_{IIR}/k_0	0.0413

TABLE 2. *Normalized stress intensity factors for a circumferential inner edge crack of the hollow finite cylinder* ($R_o = 2R_i, h = 1.5R_i$)

Magnesium				
$r_f = 1.4R_i$	k_I/k_0	0.1017	k_{II}/k_0	0.0347
$r_f = 1.5R_i$	k_I/k_0	0.0947	k_{II}/k_0	0.0376
Cadmium				
$r_f = 1.4R_i$	k_I/k_0	0.0691	k_{II}/k_0	0.0327
$r_f = 1.5R_i$	k_I/k_0	0.0612	k_{II}/k_0	0.0358

cylinder of a transversely isotropic material. All the material properties used for the following examples are given in Table 1 of part I of the paper.

Example 1. In this example a cracked short finite hollow cylinder with length $2h = 3R_i$ and outer radius of $R_o = 2R_i$ is considered. The cylinder is subjected to two self-equilibrating distributed tractions as depicted in Fig. 2 ($\tau_1 = \tau_2 = \tau_0$). The cylinder has an axisymmetric annular crack located at $z = 0.5h$. Stress intensity factors are normalized by $k_0 = \tau_0\sqrt{R_o}$, and the numerical results are reported in Table 1. The results are for two different crack lengths ($0.6R_i, 0.8R_i$) and two materials (magnesium and cadmium). Obviously, we see an increase in the normalized stress intensity factor with crack length growth. Also Mode I stress intensity factor of crack tips for magnesium is bigger than that for cadmium, while Mode II stress intensity factors behave reversely.

Example 2. The fourth example is allocated to the problem of a cracked finite hollow cylinder similar to previous example. The cylinder is weakened by a circumferential inner edge crack. The loading is also similar to former example, and the crack is also located at $z = 0.5h$. The Modes I and II normalized stress intensity factors k_I/k_0 and k_{II}/k_0 are tabulated in Table 2. One observes that Modes I and II stress intensity factors of crack tips for magnesium are bigger than those for cadmium.

Example 3. As a last example we consider a finite hollow cylinder analogous to examples 1 and 2 while it is weakened by two axisymmetric cracks. Under the action of the similar loading of previous two examples, the interaction of two coplanar cracks are studied. They are located at $z = 0.5h$. The cracks are an axisymmetric annular crack with inner and outer radii r_{sa} and r_{fa}, respectively, and an inner circumferential edge crack with tip radius r_{fc}. The results for Modes I and II normalized stress intensity factors k_I/k_0 and k_{II}/k_0 are presented in Table 3. Generally speaking, k_I/k_0 and k_{II}/k_0 for all tips of cracks are almost increased with increasing crack length. There is an exception for this characteristic. For an inner circumferential edge crack k_I/k_0 it initially experiences some increase and then decreases by crack length growth. This trend can be realized for a finite cylinder made from both materials, i.e., magnesium and cadmium. Also interaction of two adjacent crack tips has also crucial effect on increase in the stress intensity factors.

TABLE 3. *Normalized stress intensity factors for a circumferential inner edge crack and an axisymmetric annular crack of the hollow finite cylinder* ($R_o = 2R_i, h = 1.5R_i$)

Magnesium				
$r_{ia} = 1.45R_i$	k_{IL}/k_0	0.0030	k_{IIL}/k_0	0.0002
$r_{fa} = 1.55R_i$	k_{IR}/k_0	0.0065	k_{IIR}/k_0	0.0005
$r_{fc} = 1.05R_i$	k_I/k_0	0.1244	k_{II}/k_0	0.0250
$r_{ia} = 1.4R_i$	k_{IL}/k_0	0.0005	k_{IIL}/k_0	0.0024
$r_{fa} = 1.6R_i$	k_{IR}/k_0	0.0105	k_{IIR}/k_0	0.0029
$r_{fc} = 1.1R_i$	k_I/k_0	0.1293	k_{II}/k_0	0.0369
$r_{ia} = 1.35R_i$	k_{IL}/k_0	0.0108	k_{IIL}/k_0	0.0072
$r_{fa} = 1.65R_i$	k_{IR}/k_0	0.0139	k_{IIR}/k_0	0.0069
$r_{fc} = 1.15R_i$	k_I/k_0	0.1239	k_{II}/k_0	0.0397
$r_{ia} = 1.3R_i$	k_{IL}/k_0	0.0366	k_{IIL}/k_0	0.0178
$r_{fa} = 1.7R_i$	k_{IR}/k_0	0.0162	k_{IIR}/k_0	0.0134
$r_{fc} = 1.2R_i$	k_I/k_0	0.1226	k_{II}/k_0	0.0420
Cadmium				
$r_{ia} = 1.45R_i$	k_{IL}/k_0	0.0049	k_{IIL}/k_0	0.0035
$r_{fa} = 1.55R_i$	k_{IR}/k_0	0.0074	k_{IIR}/k_0	0.0036
$r_{fc} = 1.05R_i$	k_I/k_0	0.0938	k_{II}/k_0	0.0147
$r_{ia} = 1.4R_i$	k_{IL}/k_0	0.0034	k_{IIL}/k_0	0.0065
$r_{fa} = 1.6R_i$	k_{IR}/k_0	0.0113	k_{IIR}/k_0	0.0066
$r_{fc} = 1.1R_i$	k_I/k_0	0.1003	k_{II}/k_0	0.0253
$r_{ia} = 1.35R_i$	k_{IL}/k_0	0.0033	k_{IIL}/k_0	0.0113
$r_{fa} = 1.65R_i$	k_{IR}/k_0	0.0147	k_{IIR}/k_0	0.0106
$r_{fc} = 1.15R_i$	k_I/k_0	0.0950	k_{II}/k_0	0.0305
$r_{ia} = 1.3R_i$	k_{IL}/k_0	0.0212	k_{IIL}/k_0	0.0209
$r_{fa} = 1.7R_i$	k_{IR}/k_0	0.0175	k_{IIR}/k_0	0.0166
$r_{fc} = 1.2R_i$	k_I/k_0	0.0904	k_{II}/k_0	0.0358

5. Concluding remarks

From the assessment of the tables it can be seen that:

1. The transversely isotropic finite cylinder with two coplanar concentric cracks under shear stress on the lateral surface shows greater values for the stress intensity factors of bigger annular cracks than those for smaller ones. But for deeper circumferential edge cracks the Mode I stress intensity factor is smaller than that for shallow one. For the Mode II stress intensity factor we see an inverse trend.
2. Material isotropy of finite cylinder, crack length, crack type, and interaction of cracks are important factors affecting stress intensity factor of each crack tip.

Appendix A

$$\int_{R_i}^{R_o} rZ\left(\lambda_n r\right)\mathrm{d}r = 0\varpi_1\left(\varrho_1\eta_i, \lambda_n\right) = \int_{R_i}^{R_o} rI_0\left(\varrho_1\eta_i r\right)J_0\left(\lambda_n r\right)\mathrm{d}r$$

$$= \frac{1}{\lambda_n^2 + \varrho_1^2\eta_i^2}\{R_o\left[\varrho_1\eta_i I_1\left(\varrho_1\eta_i R_o\right)J_0\left(R_o\lambda_n\right) + \lambda_n I_0\left(\varrho_1\eta_i R_o\right)J_1\left(R_o\lambda_n\right)\right]$$

$$- R_i\left[\varrho_1\eta_i I_1\left(\varrho_1\eta_i R_i\right)J_0\left(R_i\lambda_n\right) + \lambda_n I_0\left(\varrho_1\eta_i R_i\right)J_1\left(R_i\lambda_n\right)\right]\}$$

$$
\begin{aligned}
\varpi_2\left(\varrho_1\eta_i,\lambda_n\right) &= \int_{R_i}^{R_o} rI_0\left(\varrho_1\eta_i r\right)Y_0\left(\lambda_n r\right)\mathrm{d}r \\
&= \frac{1}{\lambda_n^2+\varrho_1^2\eta_i^2}\{R_o\left[\varrho_1\eta_i I_1\left(\varrho_1\eta_i R_o\right)Y_0\left(R_o\lambda_n\right)+\lambda_n I_0\left(\varrho_1\eta_i R_o\right)Y_1\left(R_o\lambda_n\right)\right] \\
&\quad - R_i\left[\varrho_1\eta_i I_1\left(\varrho_1\eta_i R_i\right)Y_0\left(R_i\lambda_n\right)+\lambda_n I_0\left(\varrho_1\eta_i R_i\right)Y_1\left(R_i\lambda_n\right)\right]\} \\
\varpi_3\left(\varrho_1\eta_i,\lambda_n\right) &= \int_{R_i}^{R_o} rK_0\left(\varrho_1\eta_i r\right)J_0\left(\lambda_n r\right)\mathrm{d}r \\
&= -\frac{1}{\lambda_n^2+\varrho_1^2\eta_i^2}\{R_o\left[\varrho_1\eta_i K_1\left(\varrho_1\eta_i R_o\right)J_0\left(R_o\lambda_n\right)-\lambda_n K_0\left(\varrho_1\eta_i R_o\right)J_1\left(R_o\lambda_n\right)\right] \\
&\quad - R_i\left[\varrho_1\eta_i K_1\left(\varrho_1\eta_i R_i\right)J_0\left(R_i\lambda_n\right)-\lambda_n K_0\left(\varrho_1\eta_i R_i\right)J_1\left(R_i\lambda_n\right)\right]\} \\
\varpi_4\left(\varrho_1\eta_i,\lambda_n\right) &= \int_{R_i}^{R_o} rK_0\left(\varrho_1\eta_i r\right)Y_0\left(\lambda_n r\right)\mathrm{d}r \\
&= -\frac{1}{\lambda_n^2+\varrho_1^2\eta_i^2}\{R_o\left[\varrho_1\eta_i K_1\left(\varrho_1\eta_i R_o\right)Y_0\left(R_o\lambda_n\right)-\lambda_n K_0\left(\varrho_1\eta_i R_o\right)Y_1\left(R_o\lambda_n\right)\right] \\
&\quad - R_i\left[\varrho_1\eta_i K_1\left(\varrho_1\eta_i R_i\right)Y_0\left(R_i\lambda_n\right)-\lambda_n K_0\left(\varrho_1\eta_i R_i\right)Y_1\left(R_i\lambda_n\right)\right]\}
\end{aligned}
\tag{A.1}
$$

References

[1] Wei, X.X., Chau, K.T.: Analytic solution for finite transversely isotropic circular cylinders under the axial point load test. J. Eng. Mech. **128**(2), 209–219 (2002)

[2] Hassani, A.R., Faal, R.T., Noda, N.A.: Torsion analysis of finite solid circular cylinders with multiple concentric planar cracks. ZAMM J. Appl. Math. Mech. **97**(4), 458–472 (2017)

[3] Hills, D.A., Kelly, P., Dai, D., Korsunsky, A.: Solution of Crack Problems: The Distributed Dislocation Technique. Springer, Berlin (2013)

M. Pourseifi
Faculty of Engineering
University of Imam Ali
Tehran
Iran
e-mail: m_pourseifi@yahoo.com

R. T. Faal
Faculty of Engineering
University of Zanjan
P. O. Box 45195-313 Zanjan
Iran
e-mail: faal92@yahoo.com

E. Asadi
Department of Mechanical Engineering
University of Memphis
Memphis TN 38152
USA
e-mail: easadi@memphis.edu

(Received: March 22, 2017)